



Disruption of constitutive CXCR4 oligomers impairs oncogenic properties in lymphoid neoplasms

Simon Mobach^{a,b,c,1} , Nick D. Bergkamp^{a,1} , Ziliang Ma^{d,e,1} , Marco V. Haselager^{b,c,f} , Stephanie M. Anbuhl^{a,g}, Daphne Jurriens^h, Jelle van den Bor^a , Ziming Wang^{ij}, Caitrin Crudden^a, Jamie L. Roos^{b,c,f} , Claudia V. Perez Almeria^a , Rick A. Boergonje^a, Martin J. Lohse^{ij} , Reggie Bosma^a, Eric Eldering^{c,f,k,l} , Marco Siderius^a , Wei Wu^{d,e,m}, Marcel Spaargaren^{c,n,o} , Sanne H. Tonino^{b,c}, Arnon P. Kater^{b,c}, Martine J. Smit^{a,2} , and Raimond Heukers^{a,g,2}

Affiliations are included on p. 10.

Edited by Robert Lefkowitz, HHMI, Durham, NC; received November 21, 2024; accepted April 4, 2025

The chemokine receptor CXCR4 is overexpressed in many cancers and contributes to pathogenesis, disease progression, and resistance to therapies. CXCR4 is known to form oligomers, but the potential functional relevance in malignancies remains elusive. Using a nanobody-based BRET method, we demonstrate that oligomerization of endogenous CXCR4 on lymphoid cancer cell lines correlates with enhanced expression levels. Specific disruption of CXCR4 oligomers reduced basal cell migration and prosurvival signaling via changes in the phosphoproteome, indicating the existence of constitutive CXCR4 oligomer-mediated signaling. Oligomer disruption also inhibited growth of primary CLL 3D spheroids and sensitized primary malignant cells to clinically used Bcl-2 inhibitor venetoclax. Given its limited efficacy in some patients and the ability to develop resistance, sensitizing malignant B cells to venetoclax is of clinical relevance. Taken together, we established a noncanonical and critical role for CXCR4 oligomers in lymphoid neoplasms and demonstrated that their selective targeting has clinical potential.

leukemia | CXCR4 | receptor oligomerization | drug sensitization

The treatment landscape of B cell malignancies like chronic lymphocytic leukemia (CLL) has undergone significant transformations after the introduction of effective oral targeted therapies such as BTK-, PI3K-, and Bcl-2 inhibitors (venetoclax) and next-generation anti-CD20 monoclonal antibodies (1). Nevertheless, the unresponsiveness of some patients, along with acquired resistance and the nearly universal subsequent relapse of the disease, underscores the ongoing need for a potentially curative treatment (2). The chemokine receptor CXCR4 is overexpressed in many human cancers, including lymphoid neoplasms. In these disease states, CXCR4 induces signaling that promotes tumor survival and metastasis upon activation by its endogenous ligand CXCL12 (3). In CLL, CXCR4 was shown to promote a protective tumor microenvironment by allowing migration into the lymph node and altering the behavior of adjacent cells to support tumor survival and growth (4). CXCR4 signaling also drives the retention of malignant cells in the bone marrow, thereby protecting these cells from chemotoxic stress and targeted therapies administered (5–7). These observations support a central critical role for CXCR4 signaling in the biology of lymphoid neoplasms and position CXCR4 as an important drug target to treat such diseases (8, 9).

CXCR4 belongs to the class A G protein-coupled receptors (GPCRs). Since GPCRs regulate numerous (patho-)physiological processes and are highly amenable to drug intervention, they represent a major class of drug targets (10). Although classically perceived as monomeric signaling units, GPCRs are increasingly recognized to exist and signal as dimers or as higher-order oligomeric complexes (11). For example, it is well established that the functionality of class C GPCRs is critically dependent on the formation of homo- and heterodimers (12, 13). In contrast, the role of oligomerization in regulating receptor function and influencing downstream signaling outcomes remains unclear for the larger class A GPCR family. Some class A GPCRs appear to form transient dimers and higher-order oligomers (14, 15). However, the physiological roles of such complexes remain poorly understood to date.

A large body of evidence indicates that CXCR4 is capable of forming dimers and higher-order oligomers (i.e., clusters of three or more receptors) (16–25). Upon recombinant overexpression to levels mimicking an oncogenic setting, CXCR4 exists almost exclusively as dimers or higher-order oligomers (18, 19). In malignant lymphocytic T-cells, CXCR4 mainly resides in higher-order oligomers while it is largely monomeric in primary healthy T-cells (24), thus suggesting that CXCR4 oligomers exist and contribute to malignancy. Moreover, CXCL12-mediated migration of CXCR4-expressing T-cells was reported to be dependent on enhanced higher-order oligomer formation (24, 26), illustrating that

Significance

Class A GPCRs, including the chemokine receptor CXCR4, can form oligomers, but their functional relevance remains poorly understood. This study provides evidence for the role of constitutive CXCR4 oligomers in lymphoid neoplasms, where they drive prosurvival signaling, migration, and tumor growth. We developed a nanobody-based BRET method to demonstrate that endogenous CXCR4 constitutively oligomerizes in lymphoid cancer cells, correlating with receptor expression levels. Pharmacological disruption of these oligomers reduces tumor-associated signaling, impairs spheroid growth, and sensitizes patient-derived malignant cells to the apoptosis-inducing drug venetoclax. Since CXCR4 is frequently overexpressed and potentially clustered in various malignancies, this work offers broader implications for enhancing treatment efficacy, overcoming drug resistance, and potentially reducing side effects across multiple cancer types.

This article is a PNAS Direct Submission.

Copyright © 2025 the Author(s). Published by PNAS. This article is distributed under [Creative Commons Attribution-NonCommercial-NoDerivatives License 4.0 \(CC BY-NC-ND\)](https://creativecommons.org/licenses/by-nc-nd/4.0/).

¹S.M., N.D.B., and Z.M. contributed equally to this work.

²To whom correspondence may be addressed. Email: mj.smit@vu.nl or r.heukers@vu.nl.

This article contains supporting information online at <https://www.pnas.org/lookup/suppl/doi:10.1073/pnas.2424186122/-/DCSupplemental>.

Published June 11, 2025.

CXCR4 oligomerization impacts receptor function. However, it remains to be clarified whether CXCR4 oligomerization drives malignancy. Additionally, it is important to investigate which specific protumorigenic effects of CXCR4 are associated with signaling pathways unique to receptor oligomerization.

In this study, we set out to investigate the malignant potential of CXCR4 oligomerization. Using nanobody-based bioluminescence resonance energy transfer (BRET) and direct stochastic optical reconstruction microscopy (dSTORM) single-molecule imaging, we studied CXCR4 oligomerization in a panel of lymphoid neoplasm cell lines and primary cultures. Using mass spectrometry-based phosphoproteomics, we assessed signaling downstream of CXCR4 oligomers. Specific changes at the phosphosite level led us to uncover basal cell migration, spheroid growth, and cell survival as phenotypic consequences of constitutive CXCR4 oligomer-mediated signaling. Moreover, the attenuation of these phenotypes obtained by pharmacologically disrupting CXCR4 oligomers suggests that such clusters can serve as a therapeutic target with clinical potential.

Results

Detection of Endogenous CXCR4 Oligomers Using a Nanobody-Based BRET Approach. Oligomerization of CXCR4 has been extensively studied in heterologous expression systems (18, 19). To investigate whether this also occurs in a native setting, we developed a method for the detection of untagged GPCR oligomers in living cells. Such analysis requires a detection molecule that binds to CXCR4 with high affinity, without altering the oligomeric state of the receptor or its basal receptor signaling. One of the previously

selected CXCR4-binding nanobodies (27), VUN415, displayed such properties (*SI Appendix, Table S1*). To allow the detection of CXCR4 clusters by BRET, VUN415 was either genetically fused to NanoLuciferase (NanoLuc, Nluc) or conjugated to a fluorescent dye (Fig. 1A). Close proximity of two or more receptors enables BRET between nanobody donor and acceptor constructs bound to different CXCR4 protomers, thereby providing information about the relative receptor oligomeric state. Indeed, increasing equimolar concentrations of the two nanobody fusion constructs led to a concentration-dependent, saturable increase in nanobody binding on CXCR4-overexpressing HEK293T cells (*SI Appendix, Fig. S1A*), as well as an increase in BRET ratio (Fig. 1A). This detection was CXCR4 specific, as no binding of the probes (*SI Appendix, Fig. S1A*), and therefore no BRET, was observed in CHO-K1 or CRISPR Cas9 CXCR4-knockout HEK293T cells, which both lack CXCR4 expression (*SI Appendix, Fig. S1B*). In addition, no BRET was observed in these CXCR4^{negative} models when using a fixed saturating nanobody concentration with varying donor:acceptor probe ratios (*SI Appendix, Fig. S1 C and D*). No BRET signals were observed when VUN415-ATTO565 was replaced by unlabeled VUN415 (*SI Appendix, Fig. S2*). Collectively, these results indicate our BRET approach is highly specific, quantitative, and can be used effectively to monitor the oligomerization status of CXCR4 in subsequent mechanistic experiments.

Dimerization and higher-order oligomerization of proteins can be artificially induced through fusion to FKBP-binding protein (FKBP) domains and subsequent chemical crosslinking (28). At low expression levels where CXCR4 is expected to be predominantly monomeric (18–20), a robust increase in nanobody oligomerization BRET was observed upon stimulation with crosslinker AP20187

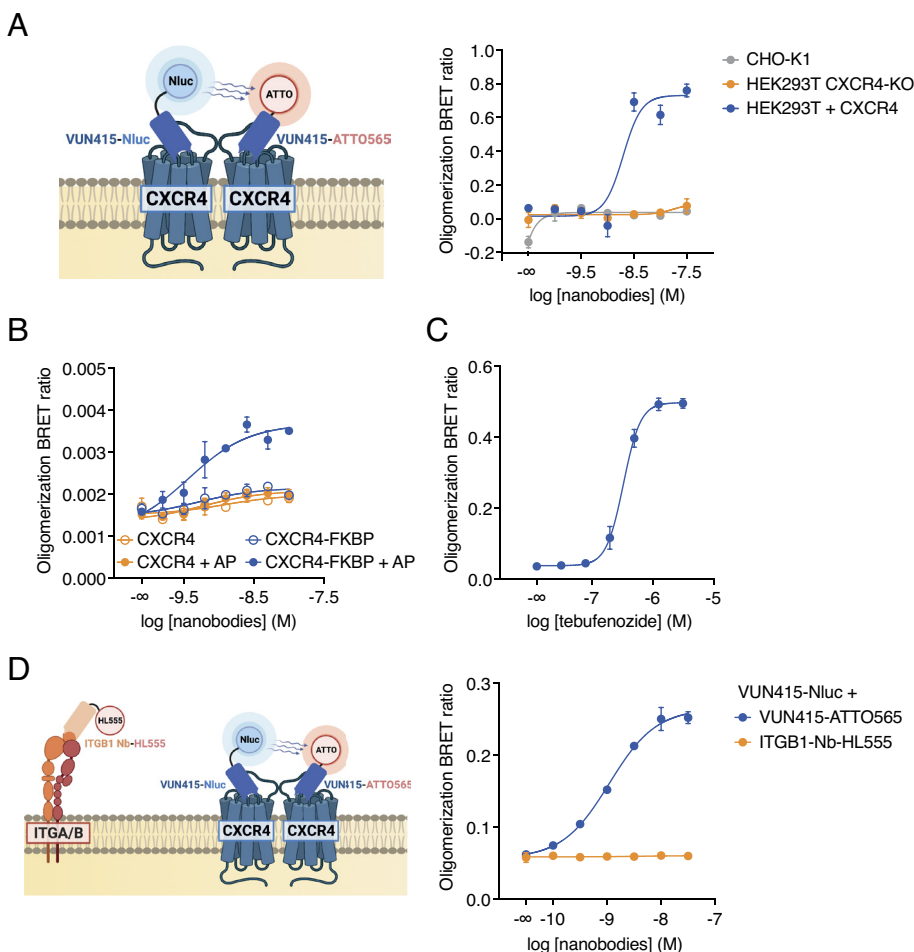


Fig. 1. Detection of endogenous CXCR4 oligomers using nanobody-based BRET. (A) Schematics and results for the nanobody-based nanoBRET method to detect receptor oligomerization in CXCR4-overexpressing HEK293T, CHO-K1, and HEK293T CXCR4 CRISPR-Cas9 KO cells. Increasing equimolar concentrations of detection nanobodies VUN415-NanoLuc (“Nluc”) and VUN415-ATTO565 were used. (B and C) Nanobody-based BRET measurement of receptor oligomerization using (B) untagged and FKBP-tagged CXCR4 or (C) ecdysone-inducible CXCR4. Stimulation with (B) 1 μ M of dimerization ligand AP20187 (“AP”) to induce dimerization or (C) increasing concentrations of tebufenozide to induce receptor expression, as indicated. (D) Schematics and data of endogenous oligomer detection in Namalwa cells using VUN415-NanoLuc (Nluc) as donor together with VUN415-ATTO565 or ITGB1-Nb-HL555 as acceptor. Data are mean \pm SD and are representative of at least three independent experiments, each performed in triplicate.

for FKBP-tagged CXCR4 and not for the untagged receptor (Fig. 1B and *SI Appendix, Fig. S3*). This shows that increased BRET values observed with our nanobody-based BRET approach is a consequence of receptor oligomerization. To verify that CXCR4 oligomerization depends on its expression level, as suggested previously (18, 19), an ecdysone-inducible CXCR4 expression construct was generated (29). Stimulation with ecdysone agonist tebufenozide indeed led to a concentration-dependent increase in CXCR4 expression, as well as nanobody-based oligomerization BRET signal (Fig. 1C and *SI Appendix, Fig. S4*).

After the initial validation of the nanobody-BRET approach in HEK293T cells, we assessed the existence of endogenous CXCR4 oligomers. We focused on lymphoid neoplasms as enhanced CXCR4 levels are considered to play a prominent pathological role (30–32). Using the Namalwa Burkitt lymphoma cell line as a proof-of-concept, we observed a robust increase in BRET signal in cells treated with CXCR4 detection nanobodies, whereas no BRET occurred when combining VUN415-Nluc with a fluorescently labeled nanobody against the highly expressed integrin $\beta 1$ (Fig. 1D). The lack of BRET for the integrin $\beta 1$ control was not due to a lack of nanobody

binding, as clear concentration-dependent binding to Namalwa cells was observed (*SI Appendix, Fig. S5*). Hence, our nanobody-based BRET approach specifically showed the presence of heterologously and endogenously expressed CXCR4 oligomers.

Enhanced Oligomerization of Endogenous CXCR4 on Lymphoid Cancer Cell Lines. Subsequently, we assessed whether CXCR4 oligomerization is associated with elevated expression of endogenous receptors on cancer cells. First, concentration–response curves for nanobody-based oligomerization detection were generated for a small selection of lymphoid cancer cell lines with varying CXCR4 expression levels and disease subtypes (Fig. 2A and *SI Appendix, Fig. S6*). In the CLL cell line MEC-1 with very low CXCR4 expression, no oligomerization BRET signal was detected, confirming specificity of the BRET assay for cells other than the HEK293T CXCR4 CRISPR Cas9 KO and CHO-K1 cells. We observed concentration-dependent increases in BRET signal for CXCR4^{low} RPC1-WM1 (Waldenstrom macroglobulinemia) cells and CXCR4^{high} Z-138 (mantle cell lymphoma, MCL) cells, with similar BRET₅₀ but much higher BRET_{max} values for the

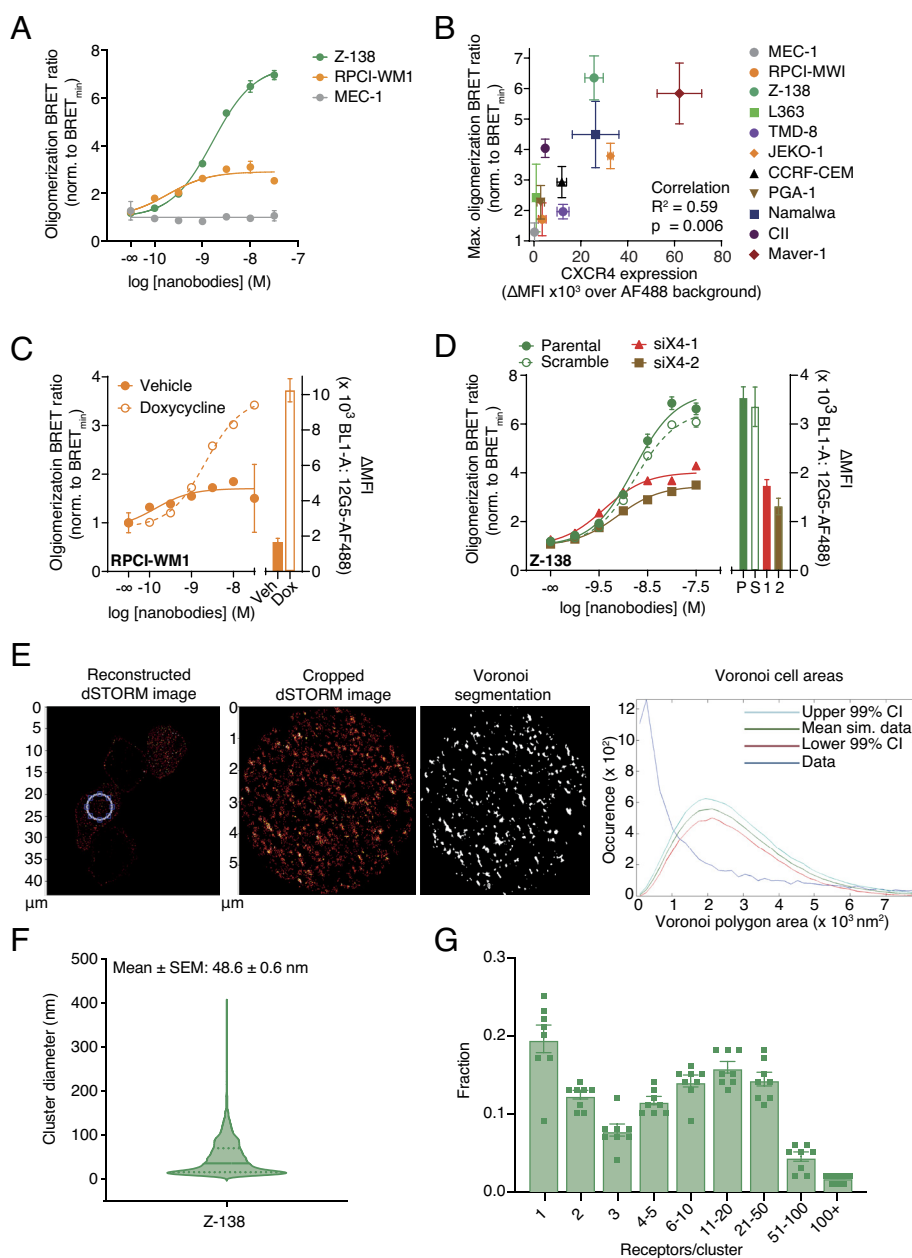


Fig. 2. Differential oligomerization of endogenous CXCR4 receptors in lymphoid cancer cell lines. (A) Nanobody-based BRET measurement of CXCR4 oligomerization in lymphoid cancer cell lines MEC-1, RPC1-WM1, and Z-138. Data are representative of at least three independent experiments and depicted as mean \pm SD. (B) Normalized CXCR4 oligomerization BRET_{max} plotted against flow cytometry surface receptor expression levels for the lymphoid cancer cell line panel. Data are pooled mean \pm SEM of at least three independent experiments, each performed in triplicate. (C and D) Effects on nanobody-based receptor oligomerization BRET of enhanced CXCR4 expression using doxycycline-inducible CXCR4 in RPC1-WM1 cells (C) or silencing of CXCR4 using scramble shRNA or CXCR4-targeting siRNA in Z-138 cells (D). Oligomerization data, normalized to the BRET_{min} value of each individual cell line, are representative of at least three independent experiments and depicted as mean \pm SD. Expression data, corrected for AF488 background, are depicted as mean \pm SEM of at least three independent experiments. (E) Data of dSTORM imaging and spatial point distribution analysis using Voronoi segmentation on Z-138 (CXCR4^{high}) cells. Full reconstructed dSTORM image and analyzed region of image (“Cropped dSTORM”), indicated by the blue circle, are visualized. Corresponding thresholded binary map and Voronoi polygon area plot are shown. In Voronoi polygon area plot, the blue line indicates the obtained data, whereas 99% CI of Monte-Carlo simulation are indicated by red and light blue lines. Representative analysis of two independent experiments is shown. (F) Cluster diameter for Z-138 cells is displayed based on the spatial point distribution analysis. Data (violin plot) are pooled from eight analyzed areas, obtained from two independent experiments per cell line. Dashed lines represent quartiles, and the solid line represents the median. (G) Cluster stoichiometry analysis of Z-138 cells. Data are pooled mean \pm SEM of eight analyzed areas, obtained from two independent experiments per cell line.

latter. Although different plate reader gain settings were used between cell lines, this did not affect the transformed $BRET_{max}$ values (*SI Appendix, Fig. S7*) and can therefore be considered to accurately reflect relative oligomerization levels. Out of a large and diverse panel of lymphoid neoplasms, oligomeric complexity of endogenous CXCR4 generally correlated with the receptor expression levels (Fig. 2*B*). Notably, some cell lines exhibited higher oligomeric complexity than expected based on their expression level, including cell lines PGA-1, L363, and CII. These deviations could be explained by other factors influencing oligomeric complexity, including membrane lipid composition (33, 34).

Of the tested cell lines, Z-138 and Maver-1 stood out as cell lines with the highest level of CXCR4 oligomers (Fig. 2*B* and *SI Appendix, Fig. S6*). To further investigate the link between receptor expression and oligomerization, we tested the effects of genetic manipulations of CXCR4 expression on CXCR4 oligomerization. Doxycycline-inducible expression of CXCR4 enhanced its oligomeric state in RPC1-WM1 (Fig. 2*C*) and MEC-1 cells (*SI Appendix, Fig. S8A*), whereas siRNA-mediated silencing of CXCR4 caused a marked reduction of endogenous receptor oligomerization in Z-138 (Fig. 2*D*) and Namalwa cells (*SI Appendix, Fig. S8B*). These data effectively demonstrate that CXCR4 expression is an important driver of receptor oligomerization in endogenous systems.

To validate the BRET-based findings of endogenous CXCR4 oligomerization, we employed dSTORM single-molecule imaging (35), using AlexaFluor™ 647-conjugated VUN415 (VUN415-AF647), on CHO-K1 (CXCR4^{negative}) and Z-138 (CXCR4^{high}) cells. To assess the specificity of VUN415-AF647, samples were incubated with an excess of CXCR4 antagonist AMD3100, which is known to displace VUN415 but does not affect CXCR4 oligomerization (19) (*SI Appendix, Fig. S9 A and B*). VUN415 can be competed off by small molecule CXCR4 binding compound AMD3100. Z-138 cells contained specific localized events as demonstrated by their elevated number compared to the corresponding nonspecific localized events in the AMD3100-treated sample (*SI Appendix, Fig. S9B*).

Next, we performed a statistical cluster analysis based on Ripley's K function, Voronoi segmentation, and localization output to analyze the CXCR4 cluster stoichiometry on Z-138 cells. Voronoi segmentation was applied to the obtained spatial distribution patterns of the localized events and compared to random distributions generated by Monte-Carlo simulations (Fig. 2*E*). Z-138 cells showed significant clustering of CXCR4 receptors (Fig. 2*E*). The average CXCR4 cluster diameter was 48.6 ± 0.6 nm (Fig. 2*F*). Cluster stoichiometry analysis showed a large population of higher-order CXCR4 oligomers (Fig. 2*G*). Collectively, these dSTORM findings validate the existence of endogenous CXCR4 oligomers detected by BRET and provide stoichiometric insights into the organization of CXCR4 into multimeric structures in lymphoid cancer cells.

Pharmacological Disruption of Endogenous CXCR4 Oligomers.

In order to investigate a potential function of CXCR4 clusters, we sought to disrupt these clusters and investigate the resulting functional consequences. Previously, we and others have shown that the inverse agonistic minor pocket-binding small molecule IT1t, inverse agonistic peptide TC14012 as well as the antagonistic N-terminus-binding nanobody VUN401, can disrupt CXCR4 oligomers (18, 19). Because completely different types of molecules (small molecule, peptide, and nanobody) are able to exert similar effects on CXCR4 oligomers and associated downstream signaling, we wondered whether other CXCR4 ligands displayed a similar mode of action. The identification of other, different oligomer-disruptors would reduce the chance that the phenotypic observations can be attributed to nonspecific IT1t

and VUN401 effects. First, we evaluated the effects of clinical candidates AMD070 (AMD11070, mavorixafor) and TG-0054 (burixafor) on CXCR4 oligomerization by assessing changes in BRET between Rluc- and YFP-tagged CXCR4 in HEK cells (Fig. 3*A*) and spatial intensity distribution analysis (SpIDA, Fig. 3*B*). In both assays, AMD070, IT1t and VUN401 reduced the CXCR4 oligomerization, whereas TG-0054 did not. VUN401 and the small molecules all inhibited the binding of fluorescently labeled CXCL12 to CXCR4 (*SI Appendix, Fig. S10A*), and inhibit CXCL12-induced miniGi recruitment without inducing canonical signaling via G proteins (*SI Appendix, Fig. S10 B and C*), indicating the ligands are antagonists, not agonists.

As IT1t interfered with VUN415 binding to CXCR4 (Fig. 3*C* and *SI Appendix, Fig. S11*), VUN415 cannot be used to monitor endogenous modulation of CXCR4 clustering by IT1t. Fortunately, out of a panel of different CXCR4-binding nanobodies, VUN416 binding was unaffected by IT1t and did not modulate CXCR4 oligomerization itself (Fig. 3*D* and *SI Appendix, Table S1*). This makes VUN416 a suitable candidate to be engineered into a BRET sensor for the assessment of the effects of IT1t on endogenous CXCR4 oligomers. A mix of VUN416-NanoLuc and VUN416-ATTO565 was able to detect endogenous CXCR4 oligomers in Z-138 cells, the lymphoid cancer cell line with the highest CXCR4 oligomeric state (Fig. 3*E*). More importantly, while IT1t did not affect the binding of these probes (*SI Appendix, Fig. S11B*), it completely abolished the oligomer BRET values (Fig. 3*E*). Fortunately, AMD070 did not affect the CXCR4 binding of oligomer detection nanobody VUN415 (*SI Appendix, Fig. S11C*), allowing the probing of endogenous oligomer disruption by this ligand. Without affecting the binding of the detection nanobodies, AMD070 indeed partially reduced the endogenous CXCR4 oligomers in Z-138 cells (Fig. 3*F*). This indicates that the oligomer-disrupting activity of IT1t and to a smaller extent AMD070 is also apparent in highly CXCR4-expressing Z-138 cells.

Constitutive CXCR4 Oligomers Drive Basal Cell Migration and Antiapoptotic Signaling in MCL Cells.

To investigate the functional consequences of CXCR4 oligomerization, we first examined the effect of CXCR4 monomerizing small molecule IT1t and nanobody VUN401 on the phosphoproteome of Z-138 cells. Because these cells display the largest CXCR4 oligomerization status, we expect to find the largest changes in protein phosphorylation upon CXCR4 oligomer disruption in these cells. By phospho-enrichment, as described previously (36), we identified a total of 15,563 phosphopeptides (purity >80%) (Fig. 4*A*). This enabled highly sensitive and specific quantifications to be performed across >15,000 phosphosites (localization probability >0.75; Class I), and between cells treated with cluster-disrupting agents and untreated controls (Fig. 4*A* and *SI Appendix, Fig. S12*). Extensive coverage of the phosphoproteome enabled an unbiased and deep characterization of phosphorylation events following CXCR4 cluster disruption, which we subsequently used as a proxy to decipher cellular impact and molecular consequences of interfering with CXCR4 cluster formation.

We found that disruption of CXCR4 oligomers changed phosphosites of cell migration mediators, such as the Rac1 effector protein serine/threonine-protein kinase PAK2, GTPase-activating protein DOCK7, and several cytoskeleton rearranging proteins. These phosphoproteins, known to regulate cell migration and reorganize the cytoskeleton, are significantly changed in the signaling pathway regulated by Rho GTPase (Fig. 4*B* and *SI Appendix, Fig. S12C*). Previously, CXCL12-induced formation of CXCR4 higher-order oligomers has been reported to be essential for sensing chemokine gradients and promoting directed migration of

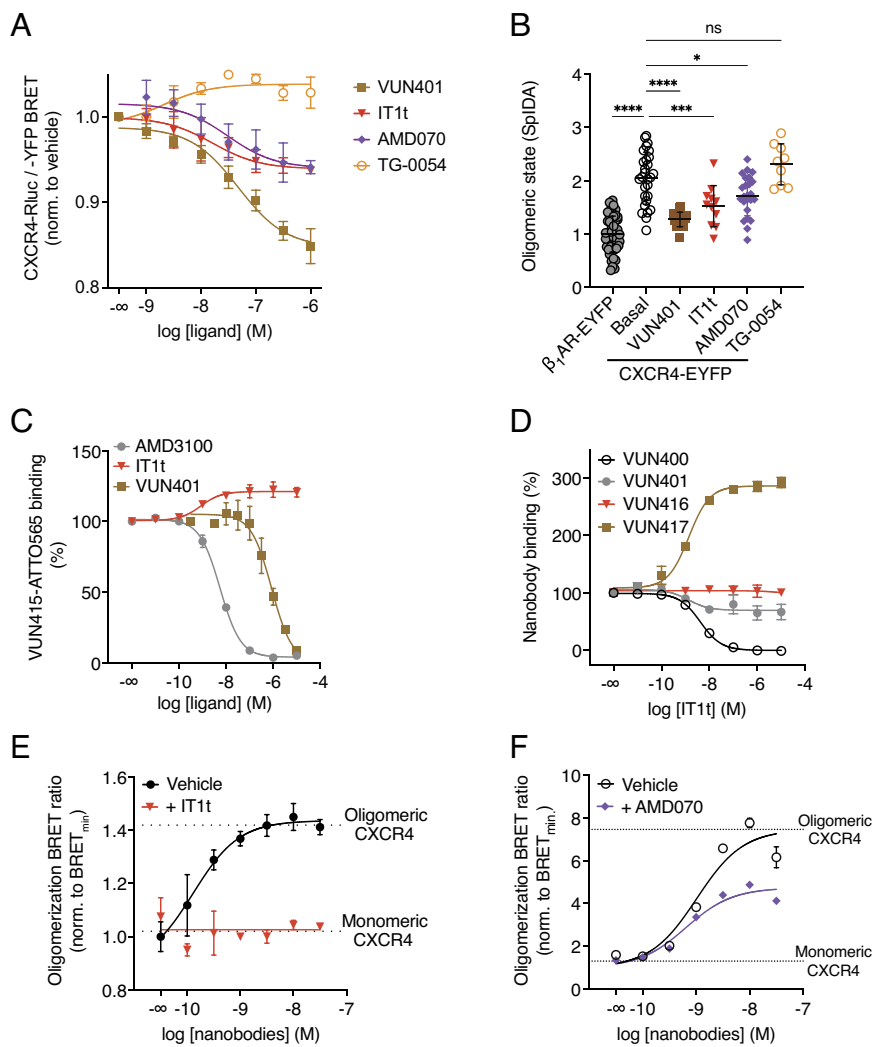


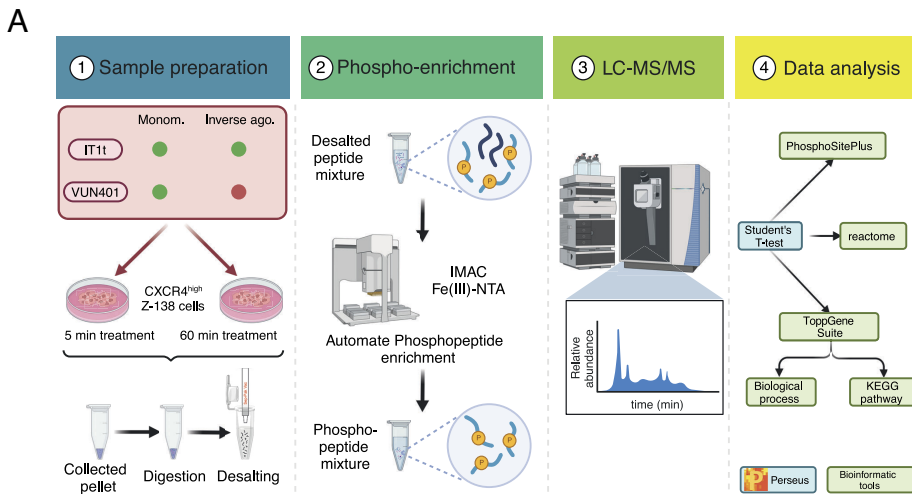
Fig. 3. The noncompetitive nanobody tool detects IT1t-induced disruption of endogenous CXCR4 oligomers in Z-138 cells. (A) Disruption of CXCR4 oligomerization by indicated concentrations of VUN401, IT1t, AMD070, or TG-0054. BRET values were determined in HEK cells expressing CXCR4-Rluc and CXCR4-YFP. Data, normalized to the buffer-only condition, are the pooled means from three experiments \pm SEM. (B) SpIDA of HEK293AD cells expressing monomeric control β_1 AR-EYFP (gray), unbound CXCR4-EYFP (white), or CXCR4-EYFP bound to VUN401 (10 μ M, brown), IT1t (10 μ M, red), AMD070 (10 μ M, purple), or TG-0054 (10 μ M, orange). Data are the mean \pm SD, with each data point representing a brightness value from one cell normalized to the monomer control. Data were obtained from three experiments per condition. **** P < 0.01, *** P < 0.001, ** P < 0.0001 compared to vehicle, according to one-way ANOVA followed by Dunnett's post hoc test. (C) Levels of BRET-based measurement of VUN415-ATTO565 (1 nM) displacement by increasing concentrations of indicated CXCR4 antagonists using membrane extracts from NanoLuc-CXCR4-expressing HEK293T cells. (D) Levels of BRET-based measurement of indicated nanobody-ATTO565 (1 nM) displacement by increasing concentrations of IT1t using membrane extracts from NanoLuc-CXCR4-expressing HEK293T cells. Data are pooled mean \pm SEM of three independent experiments (C and D). (E) VUN416-based BRET measurement of CXCR4 monomerization by 10 μ M IT1t in Z-138 cells. (F) VUN415-based BRET measurement of CXCR4 monomerization by 10 μ M AMD070 in Z-138 cells. Data are mean \pm SD and are representative of three independent experiments, each performed in triplicate.

malignant T-cells (24, 34, 37). Therefore, we hypothesized that high levels of CXCR4 oligomers might instigate basal signaling toward cell migration. We performed a live-cell imaging experiment, where a consistent proportion of the control-treated cells (5 to 10%) showed significant basal cell migration during a 4-h period. Monomerizing ligands IT1t and VUN401 impaired the basal cell migration of this population significantly, whereas non-monomerizing ligands AMD3100 and VUN415 did not (Fig. 4C). When analyzing the trajectories, both IT1t and VUN401 impaired the average migration speed of the highly migratory Z-138 cell population significantly (Fig. 4D). IT1t showed significant inhibition of the average traveled distance, whereas VUN401 showed a similar trend (SI Appendix, Fig. S13). Collectively, these results highlight a role for CXCR4 oligomers in basal cell migration, which can be modulated by oligomer disruptors.

To elucidate other CXCR4 clustering-dependent phenotypes, we performed pathway analyses to identify processes similarly affected by IT1t and VUN401 treatment. Of notable interest was the shared positive regulation of the apoptotic process by both IT1t and VUN401 (Fig. 5A), exemplified by the regulation of a large cluster of phosphosites controlling apoptotic events (Fig. 5B). Due to the annotated functions of these phosphorylation sites in regulating apoptosis, and considering the large cluster of coherently regulated phosphosites pointing toward apoptosis, we examined cell viability in more detail. CXCR4 oligomer disruption by IT1t and to a lesser extent VUN401 impaired cell viability of Z-138 cells (SI Appendix, Fig. S14A). Although these data hint

toward a protective role for basal CXCR4 oligomer-mediated signaling in these cells, the observed effects were marginal.

Therefore, we tested whether CXCR4 monomerization would increase the sensitivity of Z-138 cells to cell death. Venetoclax, a selective Bcl-2 inhibitor, is a cell-death-inducing agent that is approved for CLL and AML patients (38, 39). Cotreatment of Z-138 cells with monomerizing ligands IT1t and, to a lesser extent, VUN401 enhanced the sensitivity for venetoclax-induced cell death, as determined by measuring cell metabolic activity with a resazurin assay (Fig. 5C, data normalized to no venetoclax condition for each CXCR4 molecule to emphasize potentiation, SI Appendix, Table S2). To evaluate whether this effect extended beyond Z-138 cells, we extended our analysis with IT1t to Maver-1, JEKO-1, and PGA-1 cells. IT1t exhibited differential effects on venetoclax sensitivity across these models, indicating a broader but context-dependent impact on Bcl2 inhibition (Fig. 5D and SI Appendix, Fig. S14B and Table S3). The effect of IT1t could be blocked by a saturating concentration of the IT1t competitor and other CXCR4 binder AMD3100 (Fig. 5E), indicating that the effect is CXCR4-specific. Dual concentration-response curves of venetoclax and IT1t revealed a dose-dependent enhancement in the sensitivity of Z-138 cells for venetoclax-induced cell death that saturated at 10 μ M IT1t (SI Appendix, Fig. S15A). As an alternative approach to disrupt CXCR4 oligomers, we lowered the CXCR4 expression by a partial knockdown of CXCR4, which also showed venetoclax sensitization (Fig. 5F). Moreover, the IT1t effect was strongly impaired upon CXCR4 knockdown



B Signaling by Rho GTPases involved in cytoskeleton reorganization and cell migration

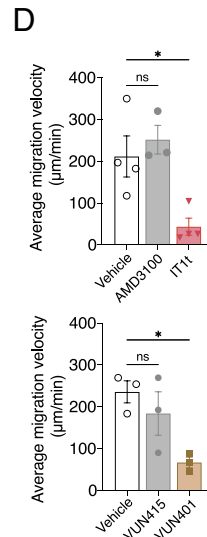
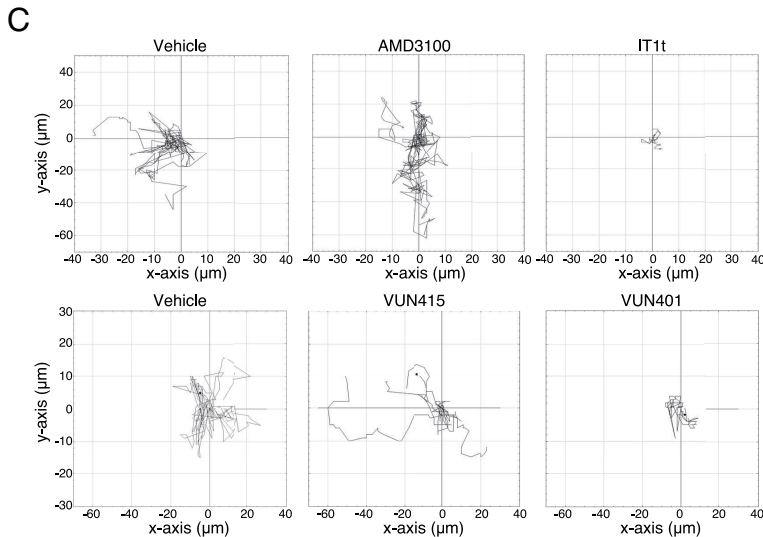
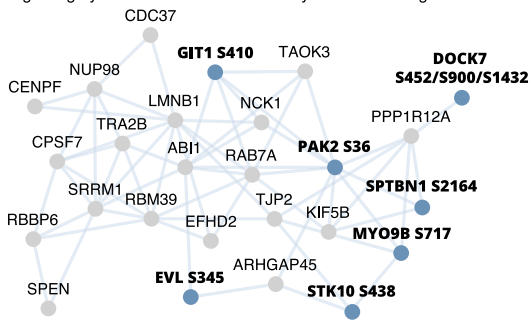


Fig. 4. CXCR4 oligomers affect basal cell migration, antiapoptotic signaling and cell viability in MCL cells. (A) Phosphoproteomics study setup and workflow. (B) Protein network of downregulated phosphoproteins in signaling by Rho GTPases involved in cytoskeleton reorganization and cell migration by 60 min of 1 μM IT1t treatment. The phosphoproteins depicted with bold text are known functional phosphosites. (C) Migration trajectory plots of MCL Z-138 cells for 4 h following treatment with 1 μM of AMD3100, IT1t, VUN415, or VUN401. Trajectories are representative of at least three independent experiments. (D) Average velocity following treatment with 1 μM of AMD3100, IT1t, VUN415, or VUN401 derived from average trajectory information. Data are pooled mean ± SEM of at least three independent experiments. * $P < 0.05$, ** $P < 0.01$ compared to vehicle, according to unpaired t tests.

(Fig. 5G and *SI Appendix*, Fig. S15B). In a FACS-based viability assay, AMD070 sensitized cells to venetoclax-induced cell death to a lesser smaller extent than IT1t, which corresponds well to its partial oligomer disrupting capability. The nonmonomerizing small molecules AMD3100 and TG-0054 did not show sensitization to venetoclax-induced cell death.

Using the Bliss independence model, a synergistic nature was observed for the enhancement of venetoclax-induced cell death of Z-138 cells by IT1t and, to a lesser extent, VUN401 (*SI Appendix*, Fig. S16A). Preincubation with the pan-caspase inhibitor qVD-OPH reduced the observed sensitization, suggesting the involvement of caspases in this process (*SI Appendix*, Fig. S16B). Collectively, these data indicate that CXCR4 clustering promotes antiapoptotic

signaling and associated phenotypes in lymphoid cancer cell lines, which can be targeted using CXCR4-monomerizing ligands

Disruption of CXCR4 Oligomerization Sensitizes to Cell Death and Inhibits Spheroid Growth in Primary CLL and MCL Cultures.

Finally, we investigated the significance of CXCR4 clusters in patient-derived primary CLL and MCL cells. Using our nanobody-BRET approach, native CXCR4 oligomers could also be detected on primary cells from five CLL patients and two MCL patients. Also, on these primary cells, the BRET values that indicate native CXCR4 oligomers could be almost completely disrupted by IT1t (Fig. 6A), similar to the results obtained with cell lines. More importantly, also in these primary CLL cultures, IT1t, but not

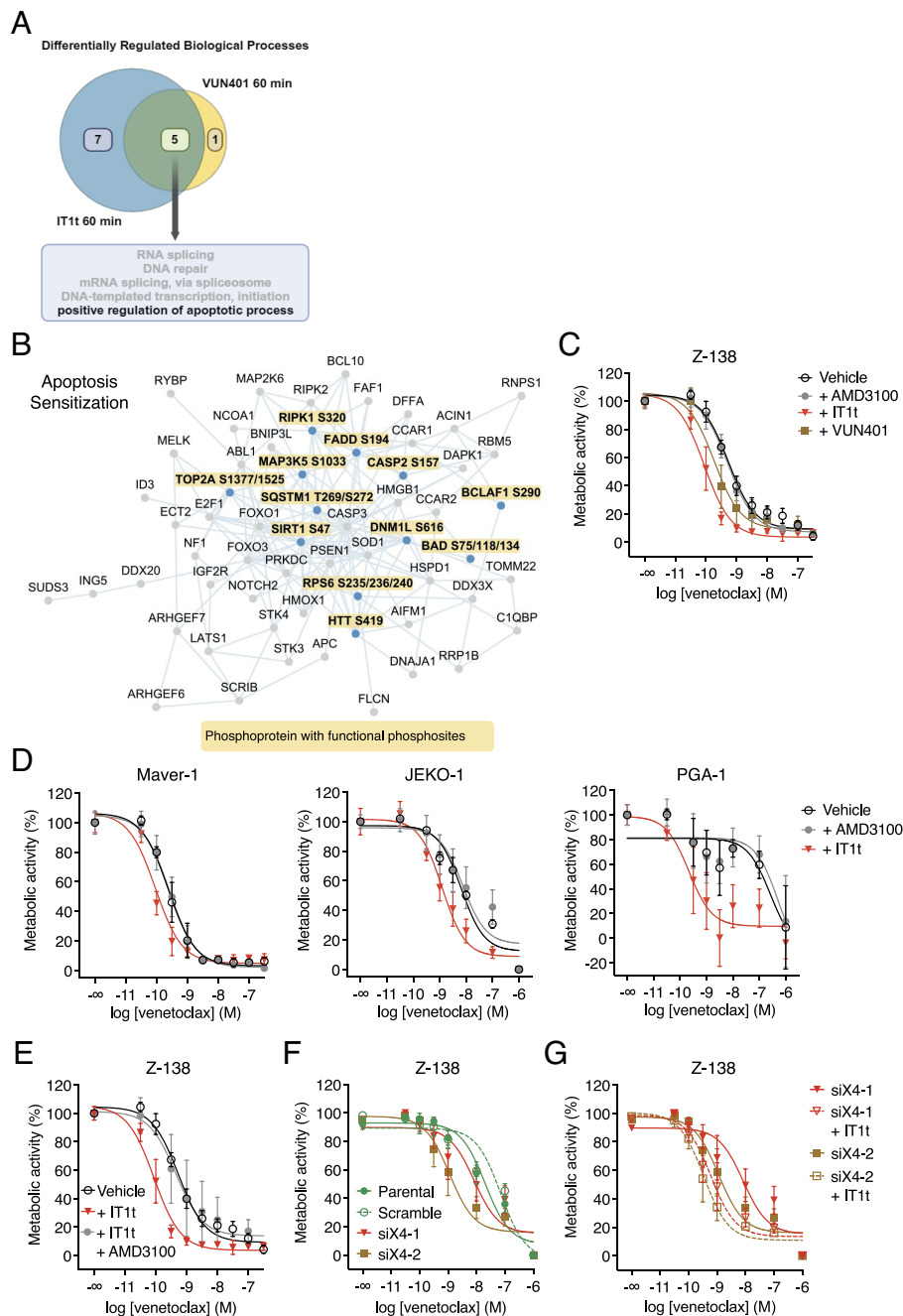


Fig. 5. CXCR4-monomerizing ligands sensitize MCL cell line Z-138 to venetoclax-induced apoptosis. (A) Venn diagram depicting overlapping and nonoverlapping GO biological processes of 1 μ M IT1t and VUN401 60-min treatment samples. (B) Protein network of downregulated phosphosites in apoptosis sensitization triggered by 60 min of 1 μ M IT1t or VUN401 treatment. The phosphoproteins depicted with bold text, in yellow rectangles, are known functional phosphosites. (C) Resazurin-based measurement of metabolic activity in Z-138 MCL cells after 48 h treatment with increasing concentrations of venetoclax in the absence (vehicle) or presence of 10 μ M AMD3100, IT1t, or VUN401. (D) Resazurin-based measurement of metabolic activity in indicated lymphoid cancer cell lines after 48 h treatment with increasing concentrations of venetoclax in the absence (vehicle) or presence of 10 μ M AMD3100 or IT1t. (E) Resazurin-based measurement of metabolic activity in Z-138 cells after 48 h treatment with increasing concentrations of venetoclax in absence (vehicle) or presence of 10 μ M IT1t \pm 100 μ M AMD3100. (F) Resazurin-based measurement of metabolic activity in Z-138 cells upon CXCR4 knockdown and 48 h treatment with increasing concentrations of venetoclax. (G) Resazurin-based measurement of metabolic activity in Z-138 cells upon CXCR4 knockdown (siX4-1 or siX4-2) and 48 h treatment with increasing concentrations of venetoclax in absence (vehicle) or presence of 10 μ M IT1t. Data, normalized to the “no venetoclax” condition, are pooled mean \pm SEM of at least three independent experiments, each performed in triplicate (C–F).

the nonmonomerizing ligand AMD3100, potentiated the effect of venetoclax (Fig. 6 B and C).

Given the importance of CXCR4 in lymph node retention (41) and the CXCR4 oligomer-driven migration we observed, we tested the effects of CXCR4 ligands in a 3D lymph node-mimicking CLL model derived from patient peripheral blood cells (40). CXCR4 monomerizers IT1t and AMD070, and not AMD3100 and TG-0054, inhibited spheroid growth without having cytotoxic effects (Fig. 6 D and E, and *SI Appendix, Figs. S17 and S18A*). Compared to AMD070, IT1t inhibited spheroid growth more potently and additionally inhibited the expression of activation marker CD25, of which expression is associated with poor disease outcome (*SI Appendix, Fig. S18B*). Taken together, our data indicate that CXCR4 oligomers also contribute to prosurvival signaling in CLL patient-derived cultures and that specific disruption of such oligomers is a promising therapeutic outlook.

Discussion

Despite major improvements in the treatment of B cell lymphoid neoplasms, many patients still experience relapsing disease that becomes more aggressive with each recurrence, characterized by acquired resistance and impaired clinical outcome. Hence, there is a need for novel therapeutic interventions, preferably targeting other signaling pathways with other modes of action. In this work, we have uncovered that CXCR4 oligomers exist on many B cell lymphoid cancer cells. Also, our data indicate that such oligomers can induce oncogenic signaling and that inhibiting this signaling through oligomer disruption represents a potential therapeutic strategy for the treatment of CLL, MCL, and other B cell lymphoid neoplasms.

High expression of CXCR4 is known to correlate with tumor growth, invasion, relapse, and therapeutic resistance (3). For example, in CLL patients, high CXCR4 expression is associated with reduced progression-free survival (42). The signaling output of

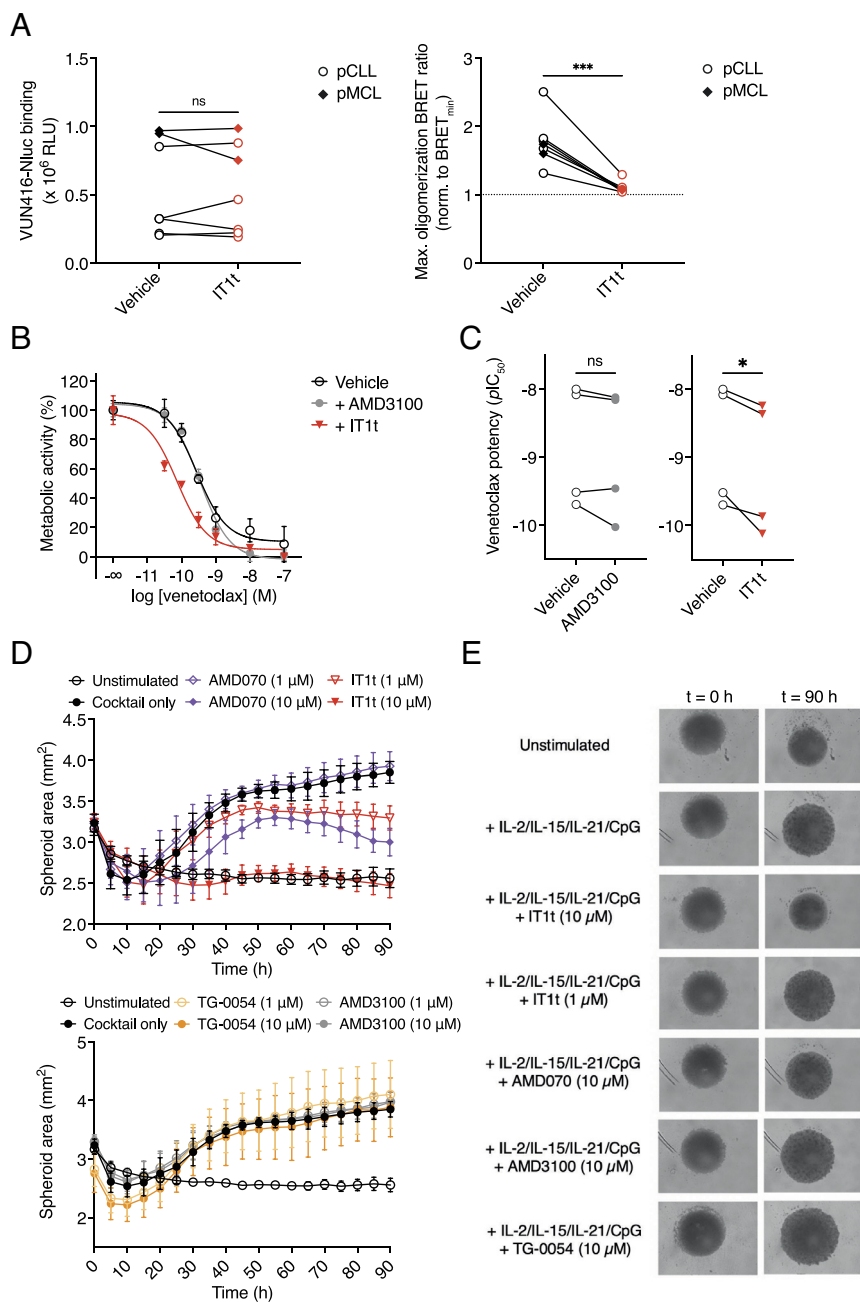


Fig. 6. Disruption of CXCR4 oligomerization sensitizes to therapy-induced cell death and inhibits spheroid growth in primary CLL and MCL cultures. (A) Effect of IT1t (10 μM) on VUN416-NanoLuc binding and nanobody-based BRET detection of CXCR4 oligomerization in PBMCs isolated from five CLL and two MCL patients. (B and C) Effects of AMD3100 and IT1t on venetoclax-induced cell death in primary cultures of CLL patients. Full concentration-response curves for one patient (B) or ΔpIC_{50} for four patients (C) are shown. (D) Effects of 1 and 10 μM of indicated CXCR4 antagonists on IL-2/IL-15/IL-21/CpG cocktail-induced growth curve in CLL patient-derived spheroid model (40). Data are mean \pm SEM of cultures from four (TG-0054) or five individual patients. (E) Effects of indicated CXCR4 antagonists on IL-2/IL-15/IL-21/CpG cocktail-induced growth curve in CLL patient-derived spheroid model after 0 and 90 h as determined by live-cell imaging (40). Representative images of a culture derived from a single patient are shown. Data are mean \pm SEM of cultures from four (TG-0054) or five individual patients. * $P < 0.05$, ** $P < 0.01$, **** $P < 0.0001$, according to unpaired t tests (A and C).

GPCRs, such as CXCR4, is generally evaluated in the context of agonist stimulation. For instance, there is ample evidence that supports the cancerous role of CXCL12-mediated migration and prosurvival signaling (3, 4, 6). However, apart from agonist-driven receptor activation, constitutive GPCR signaling exists and, in the case of CXCR4 signaling, has been reported to promote the growth and survival of acute myeloid leukemia in vivo (43). Moreover, colon cancer cells require CXCR4 expression but not ligand-induced signaling capacity for chemotherapy resistance (44). Our findings indicate that the high oligomeric state of CXCR4 in lymphoid cancer cells induces constitutive prosurvival signaling and basal migration. Similarly, the constitutive activity of breast tumor kinase and the adhesion GPCR GPR64 accelerates cell migration, contributing to tumorigenesis (45, 46). Constitutive receptor oligomerization-driven signaling has been observed for other GPCRs, as exemplified by the requirement of CCR7 oligomer formation for the interaction with and activation of tyrosine kinase Src (47). The CXCR4 oligomerization-driven basal cell

migration, likely contributing to the invasive and metastatic properties associated with this receptor, might be particularly important for cells that are not exposed to a CXCL12 gradient.

Most studies focusing on GPCR oligomerization and modulation were performed in heterologous expression systems, which may differ from endogenous systems. For instance, the M_1R antagonist pirenzepine promotes oligomerization of transfected M_1R receptors but prevents the formation of endogenous oligomers (48–50). Employing our nanobody-based tools, we report the pharmacological disruption of endogenous CXCR4 oligomers. AMD070 partially disrupted CXCR4 oligomers in lymphoid cancer cells, while IT1t appeared to induce a fully monomeric receptor state. This was slightly different in heterologous expression systems, where equal oligomer-disrupting efficacies were observed for these two small molecules. These data highlight the importance of studying oligomerization in a native context.

We have tested several small molecules for their ability to disrupt CXCR4 oligomers. Of these, AMD3100, an antagonist

lacking oligomer-disrupting properties, is used clinically for hematopoietic stem cell mobilization (51). In addition, the partial cluster disruptor AMD070 has recently been approved for the treatment of WHIM syndrome, demonstrating that antagonizing CXCR4 is clinically safe (52). In contrast to AMD3100 and TG-0054, we found that AMD070, IT1t, and nanobody VUN401 disrupted CXCR4 oligomers and inhibited downstream signaling toward cell survival and migration. The effects of IT1t could theoretically also be attributed to its ability to inhibit constitutive CXCR4-mediated $G\alpha_{i/o}$ signaling. However, VUN401 and AMD070 do not inhibit constitutive CXCR4-mediated $G\alpha_{i/o}$ signaling (19), and IT1t and VUN401 showed similar effects on antiapoptotic and cell migration signaling networks in our studies. Moreover, we recently showed that TG-0054, like IT1t, inhibited constitutive $G\alpha_i$ signaling of CXCR4, but in contrast to IT1t was not able to disrupt CXCR4 oligomeric complexes in HEK293T cells (53). This suggests inhibition of CXCR4 oligomerization to be the underlying mechanism rather than inhibition of basal $G\alpha_{i/o}$ activation.

In our venetoclax sensitization experiments and CLL patient-derived 3D spheroid model, the full monomerizing ligand IT1t was more potent and efficacious than the partial cluster disruptor AMD070. This implies that the extent to which CXCR4 oligomers can be disrupted may impact the therapeutic outcome, at least in lymphoid neoplasms. In these pathologies, high-efficacy cluster disruptors would be the most attractive candidates for the therapeutic targeting of CXCR4. As expression is a primary driver of CXCR4 oligomerization, pharmacological intervention with cluster disruptors would specifically target malignant cells that overexpress CXCR4. This would create an added layer of selectivity for targeted therapy in cancer. Our approach could be expanded to other GPCRs, like P2Y2 receptors, which are highly expressed in pancreatic cancer and form clusters that can be pharmacologically disrupted (54).

The pathological role of CXCR4 oligomerization described in this study may extend beyond the context of lymphoid neoplasms. Previously, IT1t but not AMD3100 was shown to inhibit TLR7-mediated type I interferon signaling in plasmacytoid dendritic cells from systemic lupus erythematosus patients (55). Moreover, IT1t inhibited early metastases in an *in vivo* breast cancer zebrafish model (56). Although future studies are required to investigate whether these phenotypes can be (fully) ascribed to the oligomer-disruptive effects of IT1t, this added capacity may prove beneficial over inhibiting CXCL12-induced $G\alpha_{i/o}$ signaling by antagonizing compounds like AMD3100. The therapeutic potential of inhibiting CXCR4 oligomer-mediated signaling might also be extended to other CXCR4-overexpressing cancer types. Since disruption of CXCR4 oligomers inhibited multiple hallmarks, it is not unlikely that cluster disruption can result in the potentiation of other commonly used cell-death-inducing agents.

Taken together, this study demonstrates the existence of native CXCR4 oligomers in lymphoid neoplasms and CXCR4 oligomer-driven signaling with pathophysiological importance. Selective targeting of CXCR4 clustering in lymphoid neoplasms and other cancers may have therapeutic potential on its own or by potentiating other therapeutics.

Materials and Methods

A detailed description of the *Materials and Methods* is provided in the *SI Appendix*.

DNA Constructs and Molecular Cloning. CXCR4, nanobody, reporter, and shRNA constructs were either described previously or developed as described in the *SI Appendix, Detailed Materials and Methods*.

Patient Material. All procedures involving patient material were approved by the AMC Ethical Review Biobank Board under the number METC 2013/159 and conducted in accordance with the Declaration of Helsinki.

Cell Lines and Cell Culture. Cells obtained from the American Type Culture Collection were cultured according to the provider's instructions. MEC-1, PGA-1, L363, CCRF-CEM, Jeko-1, CII, Namalwa, Maver-1, and Z-138 were described previously (57). RPCI-WM1 and TMD8 were kindly provided to Marcel Spaargaren by Dr. S.P. Treon and Dr. G. Lenz, respectively.

Nanobody Generation and Production. Nanobodies were produced in BL21 Codon+ bacteria and purified using immobilized affinity chromatography via 6x-His tags.

Fluorescent Labeling of Nanobodies. The labeling of CXCR4 nanobodies with ATTO565 fluorescent dyes (ATTO-TEC, #AD565-41, #AD565-31) using thiol-maleimide coupling and N-hydroxy-succinimide chemistry was described previously (58).

Transfection of HEK293T Cells. HEK293T cells were transfected with 25 kDa linear polyethyleneimine (PEI, Polysciences Inc.).

Receptor Oligomerization CXCR4-Rluc and CXCR4-YFP. For receptor oligomerization experiments using tagged receptors, HEK293T cells were transfected with Myc-CXCR4-Rluc and HA-CXCR4-YFP. After consecutive incubations with CXCR4 ligands and substrate coelenterazine-h, bioluminescence was measured at 475 to 30 nm and 535 to 30 nm using a PHERAstar plate reader.

CAMYEL Constitutively Active CXCR4. To assess potential inverse agonism of ligands on basal $G\alpha_{i/o}$ activation, HEK293T cells were transfected with a constitutively active CXCR4 mutant (HA-CXCR4 N119S) and CAMYEL. After consecutive incubations with CXCR4 ligands and substrate coelenterazine-h, bioluminescence was measured at 475 to 30 nm and 535 to 30 nm using a PHERAstar plate reader.

Oligomer Detection Using Nanobody-Based BRET in Transfected HEK293T Cells. To detect nanobody-based oligomerization BRET, HEK293T cells were transfected with HA-CXCR4 pcDEF3 or HA-CXCR4 pEUI. For FKBP experiments, HEK293T cells were transfected with HA-CXCR4 or HA-CXCR4-FKBP.

ELISA for Surface Expression of Ecdysone-Inducible CXCR4. CXCR4 surface expression was detected with the monoclonal mouse anti-CXCR4 antibody 12G5 and horseradish peroxidase-conjugated goat-anti-mouse antibody. Binding was determined with 1-step Ultra TMB-ELISA substrate (Thermo Fisher Scientific), and the reaction was stopped with 1M H_2SO_4 . Optical density was measured at 450 nm using a CLARIOstar plate reader.

Membrane Extract Preparation. Membrane extracts from HEK293T cells expressing NanoLuc-CXCR4 were prepared as previously described (58).

Displacement of Fluorescent Nanobodies and CXCL12. Membrane extracts from NanoLuc-CXCR4-expressing HEK293T cells and increasing concentrations of unlabeled ligands were incubated in a white flat-bottom 96-well plate. Next, fluorescent ligands were added. After the addition of substrate furimazine (NanoGlo Luciferase Assay System, Promega), luminescence was measured using a PHERAstar plate reader with 610 nm/LP and 460/80 nm filters.

Mini- $G\alpha_i$ Recruitment. To measure CXCR4-induced mini- $G\alpha_i$ recruitment, HEK293T cells were transfected with HA-CXCR4-NanoLuc and Venus-mini- $G\alpha_i$. After consecutive incubations with CXCR4 ligands and substrate furimazine, bioluminescence was measured at 475 to 30 nm and 535 to 30 nm using a PHERAstar plate reader.

cAMP Measurement. cAMP accumulation in Namalwa cells was measured using the Ultra cAMP kit (Lance) according to the manufacturer's instructions. HTRF was measured using a PHERAstar plate reader after excitation at 337 nm and emission at 620 and 665 nm.

Flow Cytometry for CXCR4 Surface Expression Determination. CXCR4 surface expression was determined using mouse anti-CXCR4 antibody 12G5 and goat anti-mouse IgG (H+L) AlexaFluor™ 488. Samples were analyzed utilizing an Attune Nxt Flow Cytometer (Thermo Fisher Scientific) at the AUMC Microscopy

Cytometry Core Facility (MCCF), and data analysis was conducted using FlowJo version 10 (BD Biosciences).

Oligomer Detection Using Nanobody-Based BRET in Lymphoid Cancer Cell Lines. CXCR4 oligomers were detected in lymphoid cancer cells and PBMCs derived from CLL patients using VUN415/VUN416-NanoLuc and VUN415/VUN416-ATTO565 or ITGB1-Nb-HL555 (QvQ). Fluorescence was measured using a CLARIOstar plate reader at 563/30 nm excitation and 592/30 nm emission. Luminescence was measured using a PHERAstar plate reader with 610 nm/LP and 460/80 nm filters after the addition of substrate furimazine.

Lentivirus Production and Transduction. MEC-1 and RPCI-WM1 cell lines with inducible HA-CXCR4 expression and Namalwa and Z-138 cell lines with constitutive siRNA CXCR4 or scramble shRNA expression were generated by lentiviral transduction, as previously described (59, 60). Knockdown efficiency and enhanced CXCR4 surface expression in the different cell lines were validated by determining CXCR4 surface expression levels as described before. CXCR4 expression in the doxycycline-inducible cell lines was induced using 1 μ g/mL doxycycline (Sigma-Aldrich).

dSTORM. Fixed samples from RPCI-WM1, Z-138, and CHO-K1 cells were stained with VUN415-AF647 and mounted in oxygen scavenger-containing Glox buffer, as previously described (61). Imaging was performed on a Ti-E microscope (Nikon) equipped with a 100x Apo TIRF oil immersion objective (NA 1.49) and Perfect Focus System 3 (Nikon). Acquired stacks were analyzed using v.1.2.1 of a custom ImageJ plugin called DoM (Detection of Molecules) (https://github.com/ekatruxha/DoM_Utrecht), as previously described (61). The acquired localization output by DoM was imported into the application ClusterViSu (<https://github.com/andronovl/SharpViSu>) that conducts a statistical cluster analysis based on Ripley's K-function and Voronoi segmentation, as previously described (62).

SpIDA. SpIDA was performed with HEK293AD cells expressing CXCR4-EYFP. Imaging was performed using a commercial laser-scanning confocal microscope (Leica SP8) equipped with a 63 \times /1.40 NA oil immersion objective, a white light laser, and photon counting hybrid detectors. For image analysis, the open-source custom-made code (<https://github.com/PaoloAnnibale/MolecularBrightness>) was loaded onto the Igor Pro software (WaveMetrics).

Phosphoproteomics. After sample preparation, phosphopeptides were enriched by automated Fe(III)-NTA. Flowthroughs and elutions were dried and injected directly into a liquid chromatography-coupled mass spectrometer. The phosphoproteome measurement was performed on an Orbitrap Exploris 480 mass spectrometer (Thermo Fisher Scientific) coupled with an UltiMate 3000 UHPLC system (Thermo Fisher Scientific). Data search was performed using MaxQuant (version 2.1.3.0) with an integrated Andromeda search engine, against the human Swiss-Prot protein database. Quantitative data filtering was conducted using the Perseus software (version 1.6.14.0).

Constitutive Cell Migration Assessment. The effect of CXCR4 ligands on the constitutive migration of Z-138 cells was tested by mixing cells with BD Matrigel™ and Ibidi μ -slide Chemotaxis (IbidiTreat surface modification), according to the manufacturer's instructions. Time-lapse video microscopy was conducted using a Nikon Ti2 microscope. Image analysis was performed using the open-source image processing software ImageJ2, version 2.14.0/1.54f. The manual tracking plugin was employed to analyze the trajectories of cells exhibiting high basal motility. The Ibidi Chemotaxis and Migration Tool ImageJ plugin was utilized to generate Rose plots and extract average trajectory information.

Resazurin Assays for Venetoclax Sensitization. Resazurin-based fluorescent cytotoxicity readouts were performed using Z-138, Jeko-1, and Maver-1 cells or PBMCs and measured using a CLARIOstar plate reader at 540/30 nm excitation and 590/30 nm emission.

FACS Viability Assays for Venetoclax Sensitization. FACS viability assays were performed with Z-138, Jeko-1, and Maver-1 cells using MitoTracker Orange (ThermoFisher Scientific, M7510) and Topro-3 (ThermoFisher Scientific, T3605) and analyzed using an Attune NxT Flow Cytometer.

Spheroid Assays. Growth of three-dimensional (3D) cultures of CLL patient-derived PBMCs was measured using an IncuCyte live-cell imager (Essen Biosciences). Spheroid area was quantified using IncuCyte software as a proxy for spheroid growth. After culture, T cell activation and viability were measured using a Canto II flow cytometer (BD Biosciences).

Data Analysis. All graphs and bar plots were visualized, and statistical analyses were performed using Prism version 10.0 (GraphPad) unless indicated otherwise. Curves were fitted using least squares nonlinear regressions, assuming a sigmoidal fit (for concentration–response curves). The significance of differences was determined as indicated in the figure legends. Schematics for assay formats were generated using Biorender.com.

Data, Materials, and Software Availability. The phosphoproteomics data have been deposited to the ProteomeXchange Consortium through the PRIDE partner repository with the dataset identifier [PXD053673](https://doi.org/10.26434/chemrxiv-2023-pxd05) (63). All other data are included in the manuscript and/or *SI Appendix*.

ACKNOWLEDGMENTS. This work was funded by the following grants: Netherlands Organization for Scientific Research Grant ENPPS.TA.019.003 MAGNETIC for S.M., N.D.B. and Z.M., M.Sp., W.W., S.H.T., A.P.K. and R.H., the ZonMw Veni Grant 09150162010212 for C.C., the ZonMw Grant 91217002 for D.J., the European Union H2020-MSCA Grant 641833-ONCORNET for M.Si., M.J.S. and R.H., H2020-MSCA Grant 860229-ONCORNET 2.0 for S.M.A., Z.W., C.V.P.A., M.J.L., M. Siderius, M.J.S. and R.H. We greatly acknowledge the Microscopy & Cytometry core facility of the Amsterdam University Medical Center for imaging and cytometry support. We greatly appreciate Prof. Dr. Lukas Kapitein for helping out with the dSTORM experiments.

Author affiliations: ¹Department of Chemistry and Pharmaceutical Sciences, Division of Medicinal Chemistry, Amsterdam Institute for Molecular and Life Sciences, Vrije Universiteit Amsterdam, Amsterdam 1081 HZ, The Netherlands; ²Amsterdam University Medical Center location University of Amsterdam, Department of Hematology, Amsterdam 1105 AZ, The Netherlands; ³Lymphoma and Myeloma Center Amsterdam, Amsterdam 1105 AZ, The Netherlands; ⁴Department of Biomolecular Mass Spectrometry and Proteomics, Biomolecular Mass Spectrometry and Proteomics, Bijvoet Center for Biomolecular Research, Utrecht University, Utrecht 3584 CH, The Netherlands; ⁵Singapore Immunology Network, Agency for Science, Technology and Research, Immunos, Singapore 138648, Republic of Singapore; ⁶Cancer Center Amsterdam, Cancer Immunology, Amsterdam 1081 HV, The Netherlands; ⁷QVQ Holding B.V., Utrecht 3584 CL, The Netherlands; ⁸Cell Biology, Neurobiology and Biophysics, Department of Biology, Faculty of Science, Utrecht University, Utrecht 3584 CH, Netherlands; ⁹Receptor Signaling Group, Max Delbrück Center for Molecular Medicine, Berlin 13125, Germany; ¹⁰ISAR Bioscience Institute, Planegg 82152, Germany; ¹¹Amsterdam University Medical Center location University of Amsterdam, Department of Experimental Immunology, Amsterdam 1105 AZ, The Netherlands; ¹²Amsterdam Institute for Infection and Immunity, Cancer Immunology, Amsterdam 1105 AZ, The Netherlands; ¹³Department of Pharmacy and Pharmaceutical Sciences, Faculty of Science, National University of Singapore, Singapore 117543, Republic of Singapore; ¹⁴Department of Pathology, Amsterdam University Medical Center location University of Amsterdam, Amsterdam 1105 AZ, The Netherlands; and ¹⁵Cancer Center Amsterdam, Cancer Biology and Immunology-Target & Therapy discovery, Amsterdam 1081 HV, The Netherlands

Author contributions: S.M., N.D.B., Z.M., M. Siderius, S.H.T., A.P.K., M.J.S., and R.H. designed research; S.M., N.D.B., Z.M., M.V.H., S.M.A., D.J., J.v.d.B., Z.W., C.C., J.L.R., C.V.P.A., and R.A.B. performed research; S.M., N.D.B., Z.M., M.V.H., S.M.A., D.J., J.v.d.B., Z.W., C.C., J.L.R., C.V.P.A., R.A.B., M.J.L., R.B., E.E., M. Siderius, W.W., M. Spaargaren, S.H.T., A.P.K., M.J.S., and R.H. analyzed data; M.J.L., E.E., M. Siderius, W.W., M. Spaargaren, S.H.T., A.P.K., and M.J.S. supervised; and S.M., N.D.B., Z.M., M. Siderius, W.W., M. Spaargaren, S.H.T., A.P.K., M.J.S., and R.H. wrote the paper.

Competing interest statement: S.M.A. and R.H. are employed by QVQ, a CRO offering Nb services and reagents. A provisional patent application has been filed on the research described in this manuscript (P135924EP00).

1. P. J. Hampel, S. A. Parikh, Chronic lymphocytic leukemia treatment algorithm 2022. *Blood Cancer J.* **12**, 161 (2022).
2. G. P. Sullivan, L. Flanagan, D. A. Rodrigues, T. Ni Chonghaile, The path to venetoclax resistance is paved with mutations, metabolism, and more. *Sci. Transl. Med.* **14**, eabo6891 (2022).
3. S. Chatterjee, B. Behnam Azad, S. Nimmagadda, The intricate role of CXCR4 in cancer. *Adv. Cancer Res.* **124**, 31–82 (2014).

4. M. J. Smit *et al.*, The CXCL12/CXCR4/ACKR3 axis in the tumor microenvironment: Signaling, crosstalk, and therapeutic targeting. *Annu. Rev. Pharmacol. Toxicol.* **61**, 541–563 (2021).
5. Y. Tesfai *et al.*, Interactions between acute lymphoblastic leukemia and bone marrow stromal cells influence response to therapy. *Leuk. Res.* **36**, 299–306 (2012).
6. A. Peled, S. Klein, K. Beider, J. A. Burger, M. Abraham, Role of CXCL12 and CXCR4 in the pathogenesis of hematological malignancies. *Cytokine* **109**, 11–16 (2018).

7. M. V. Haselager *et al.*, Changes in Bcl-2 members after ibrutinib or venetoclax uncover functional hierarchy in determining resistance to venetoclax in CLL. *Blood* **136**, 2918–2926 (2020).
8. D. Cancilla, M. P. Rettig, J. F. DiPersio, Targeting CXCR4 in AML and ALL. *Front. Oncol.* **10**, 1672 (2020).
9. R. Swanberg, S. Janum, P. E. M. Patten, A. G. Ramsay, C. U. Niemann, Targeting the tumor microenvironment in chronic lymphocytic leukemia. *Haematologica* **106**, 2312–2324 (2021).
10. A. S. Hauser, M. M. Attwood, M. Rask-Andersen, H. B. Schioth, D. E. Gloriam, Trends in GPCR drug discovery: New agents, targets and indications. *Nat. Rev. Drug Discov.* **16**, 829–842 (2017).
11. G. Milligan, R. J. Ward, S. Marsango, GPCR homo-oligomerization. *Curr. Opin. Cell Biol.* **57**, 40–47 (2019).
12. D. El Moustaine *et al.*, Distinct roles of metabotropic glutamate receptor dimerization in agonist activation and G-protein coupling. *Proc. Natl. Acad. Sci. U.S.A.* **109**, 16342–16347 (2012).
13. J. Kniazeff, L. Prézéau, P. Rondard, J.-P. Pin, C. Goudet, Dimers and beyond: The functional puzzles of class C GPCRs. *Pharmacol. Ther.* **130**, 9–25 (2011).
14. M. Bouvier, T. E. Hebert, CrossTalk proposal: Weighing the evidence for Class A GPCR dimers, the evidence favors dimers. *J. Physiol.* **592**, 2439–2441 (2014).
15. N. A. Lambert, J. A. Javitch, CrossTalk opposing view: Weighing the evidence for class A GPCR dimers, the jury is still out. *J. Physiol.* **592**, 2443–2445 (2014).
16. D. Di Marino, P. Conflitti, S. Motta, V. Limongelli, Structural basis of dimerization of chemokine receptors CCR5 and CXCR4. *Nat. Commun.* **14**, 6439 (2023).
17. J. S. Paradis *et al.*, Computationally designed GPCR quaternary structures bias signaling pathway activation. *Nat. Commun.* **13**, 6826 (2022).
18. R. J. Ward *et al.*, Chemokine receptor CXCR4 oligomerization is disrupted selectively by the antagonist ligand IT1t. *J. Biol. Chem.* **296**, 100139 (2021).
19. A. Isbilir *et al.*, Advanced fluorescence microscopy reveals disruption of dynamic CXCR4 dimerization by subpocket-specific inverse agonists. *Proc. Natl. Acad. Sci. U. S. A.* **117**, 29144–29154 (2020).
20. B. Ge *et al.*, Single-molecule imaging reveals dimerization/oligomerization of CXCR4 on plasma membrane closely related to its function. *Sci Rep.* **7**, 16873 (2017).
21. B. Wu *et al.*, Structures of the CXCR4 chemokine GPCR with small-molecule and cyclic peptide antagonists. *Science* **330**, 1066–1071 (2010).
22. J. Wang, L. He, C. A. Combs, G. Roderiquez, M. A. Norcross, Dimerization of CXCR4 in living malignant cells: Control of cell migration by a synthetic peptide that reduces homologous CXCR4 interactions. *Mol. Cancer Ther.* **5**, 2474–2483 (2006).
23. Y. Percherancier *et al.*, Bioluminescence resonance energy transfer reveals ligand-induced conformational changes in CXCR4 homo- and heterodimers. *J. Biol. Chem.* **280**, 9895–9903 (2005).
24. L. Martinez-Munoz *et al.*, Separating actin-dependent chemokine receptor nanoclustering from dimerization indicates a role for clustering in CXCR4 signaling and function. *Mol. Cell* **70**, 106–119. e110 (2018).
25. K. Saotome *et al.*, Structural insights into CXCR4 modulation and oligomerization. bioRxiv [Preprint] (2024). 10.1101/2024.02.09.579708.
26. E. M. Garcia-Cuesta *et al.*, Allosteric modulation of the CXCR4: CXCL12 axis by targeting receptor nanoclustering via the TMV-TMVI domain. *eLife* **13**, RP93968 (2024).
27. S. M. Anbuhl *et al.*, Multivalent CXCR4-targeting nanobody formats differently affect affinity, receptor clustering, and antagonism. *Biochem. Pharmacol.* **227**, 116457 (2024).
28. E. G. Hofman *et al.*, Ligand-induced EGF receptor oligomerization is kinase-dependent and enhances internalization. *J. Biol. Chem.* **285**, 39481–39489 (2010).
29. S. Lee *et al.*, Ecdysone receptor-based singular gene switches for regulated transgene expression in cells and adult rodent tissues. *Mol. Ther. Nucleic Acids* **5**, e367 (2016).
30. R. Mohle, C. Failenschmid, F. Bautz, L. Kanz, Overexpression of the chemokine receptor CXCR4 in B cell chronic lymphocytic leukemia is associated with increased functional response to stromal cell-derived factor-1 (SDF-1). *Leukemia* **13**, 1954–1959 (1999).
31. M. J. Moreno *et al.*, CXCR4 expression enhances diffuse large B cell lymphoma dissemination and decreases patient survival. *J. Pathol.* **235**, 445–455 (2015).
32. H. J. Wester *et al.*, Disclosing the CXCR4 expression in lymphoproliferative diseases by targeted molecular imaging. *Theranostics* **5**, 618–630 (2015).
33. K. Pluhackova, S. Gahbauer, F. Kranz, T. A. Wassenaar, R. A. Bockmann, Dynamic cholesterol-conditioned dimerization of the g protein coupled chemokine receptor type 4. *PLoS Comput. Biol.* **12**, e1005169 (2016).
34. S. R. Gardeta *et al.*, Sphingomyelin depletion inhibits CXCR4 dynamics and CXCL12-mediated directed cell migration in human T cells. *Front. Immunol.* **13**, 925559 (2022).
35. M. A. Kiskowski, J. F. Hancock, A. K. Kenworthy, On the use of Ripley's K-function and its derivatives to analyze domain size. *Biophys. J.* **97**, 1095–1103 (2009).
36. H. Post *et al.*, Robust, sensitive, and automated phosphopeptide enrichment optimized for low sample amounts applied to primary hippocampal neurons. *J. Proteome Res.* **16**, 728–737 (2017).
37. E. M. Garcia-Cuesta *et al.*, Altered CXCR4 dynamics at the cell membrane impairs directed cell migration in WHIM syndrome patients. *Proc. Natl. Acad. Sci. U.S.A.* **119**, e2119483119 (2022).
38. A. Vereerbrugghen *et al.*, In vitro sensitivity to venetoclax and microenvironment protection in hairy cell leukemia. *Front. Oncol.* **11**, 598319 (2021).
39. A. J. Souers *et al.*, ABT-199, a potent and selective BCL-2 inhibitor, achieves antitumor activity while sparing platelets. *Nat. Med.* **19**, 202–208 (2013).
40. M. V. Haselager *et al.*, In vitro 3D spheroid culture system displays sustained T cell-dependent CLL proliferation and survival. *Hemasphere* **7**, e938 (2023).
41. Y. Gu *et al.*, Tumor-educated B cells selectively promote breast cancer lymph node metastasis by HSPA4-targeting IgG. *Nat. Med.* **25**, 312–322 (2019).
42. X. Xue *et al.*, CXCR4 overexpression in chronic lymphocytic leukemia associates with poorer prognosis: A prospective, single-center, observational study. *Genes Immun.* **25**, 117–123 (2024).
43. R. Ramakrishnan *et al.*, CXCR4 signaling has a CXCL12-independent essential role in murine MLL-AF9-driven acute myeloid leukemia. *Cell Rep* **31**, 107684 (2020).
44. M. A. Nengroo *et al.*, CXCR4 intracellular protein promotes drug resistance and tumorigenic potential by inversely regulating the expression of death receptor 5. *Cell Death Dis.* **12**, 464 (2021).
45. M. C. Peeters *et al.*, The adhesion G protein-coupled receptor G2 (ADGRG2/GPR64) constitutively activates SRE and NFκB and is involved in cell adhesion and migration. *Cell. Signal.* **27**, 2579–2588 (2015).
46. S. Miah, A. Martin, K. E. Lukong, Constitutive activation of breast tumor kinase accelerates cell migration and tumor growth in vivo. *Oncogenesis* **1**, e11 (2012).
47. M. A. Hauser *et al.*, Inflammation-induced CCR7 oligomers form scaffolds to integrate distinct signaling pathways for efficient cell migration. *Immunity* **44**, 59–72 (2016).
48. B. Ilien *et al.*, Pirenzepine promotes the dimerization of muscarinic M1 receptors through a three-step binding process. *J. Biol. Chem.* **284**, 19533–19543 (2009).
49. J. D. Pediani, R. J. Ward, A. G. Godin, S. Marsango, G. Milligan, Dynamic regulation of quaternary organization of the M1 muscarinic receptor by subtype-selective antagonist drugs. *J. Biol. Chem.* **291**, 13132–13146 (2016).
50. S. Marsango *et al.*, The M(1) muscarinic receptor is present in situ as a ligand-regulated mixture of monomers and oligomeric complexes. *Proc. Natl. Acad. Sci. U.S.A.* **119**, e2201103119 (2022).
51. I. Pusic, J. F. DiPersio, Update on clinical experience with AMD3100, an SDF-1/CXCL12–CXCR4 inhibitor, in mobilization of hematopoietic stem and progenitor cells. *Curr. Opin. Hematol.* **17**, 319–326 (2010).
52. A. Mullard, CXCR4 chemokine antagonist scores a first FDA approval for WHIM syndrome. *Nat. Rev. Drug Discov.* **23**, 411 (2024).
53. K. S. Pan *et al.*, Pharmacological characterisation of a clinical candidate, TG-0054, a small molecule inverse agonist targeting CXCR4. *Mol. Pharmacol.* **107**, 100015 (2025).
54. M. D. Joseph, E. Tomas Bort, R. P. Grose, P. J. McCormick, S. Simoncelli, Quantitative super-resolution imaging for the analysis of GPCR oligomerization. *Biomolecules* **11**, 1503 (2021).
55. N. Smith *et al.*, Control of TLR7-mediated type I IFN signaling in pDCs through CXCR4 engagement—A new target for lupus treatment. *Sci. Adv.* **5**, eaav9019 (2019).
56. C. Tulotta *et al.*, Inhibition of signaling between human CXCR4 and zebrafish ligands by the small molecule IT1t impairs the formation of triple-negative breast cancer early metastases in a zebrafish xenograft model. *Dis. Model. Mech.* **9**, 141–153 (2016).
57. H. C. Lantermans *et al.*, Identification of the SRC-family tyrosine kinase HCK as a therapeutic target in mantle cell lymphoma. *Leukemia* **35**, 881–886 (2021).
58. J. van den Bor *et al.*, NanoB(2) to monitor interactions of ligands with membrane proteins by combining nanobodies and NanoBRET. *Cell Rep. Methods* **3**, 100422 (2023).
59. R. H. de Wit *et al.*, Human cytomegalovirus encoded chemokine receptor US28 activates the HIF-1α/PKM2 axis in glioblastoma cells. *Oncotarget* **7**, 67966–67985 (2016).
60. R. Heukers *et al.*, The constitutive activity of the virally encoded chemokine receptor US28 accelerates glioblastoma growth. *Oncogene* **37**, 4110–4121 (2018).
61. A. Chazeau, E. A. Katrukha, C. C. Hoogenraad, L. C. Kaptein, Studying neuronal microtubule organization and microtubule-associated proteins using single molecule localization microscopy. *Methods Cell Biol.* **131**, 127–149 (2016).
62. L. Andronov, I. Orlov, Y. Lutz, J. L. Vonesch, B. P. Klaholz, ClusterViSu, a method for clustering of protein complexes by Voronoi tessellation in super-resolution microscopy. *Sci Rep* **6**, 24084 (2016).
63. Z. Ma, W. Wu, Phosphoproteomics analysis for anti-apoptotic signaling driven by CXCL4 oligomerization in MCL cells. ProteomeXchange. <https://proteomecentral.proteomexchange.org/cgi/GetDataset?ID=PX0053673>. Deposited 4 July 2024.